Primary photo-events in a metastable photomerocyanine of spirooxazines

R. Sai Santosh Kumar,[1*] Larry Lüer,[2] Dario Polli,[1,3] Michele Garbugli,[3] and Guglielmo Lanzani[1,3]

[1]*Center for Nano Science and Technology of IIT@PoliMI, Via Pascoli 70/3, Milan, Italy*
[2] *Madrid Institute for Advanced Studies, IMDEA Nanociencia, Mòdulo 13, 28049 Madrid, Spain*
[3]*Dipartimento di Fisica, Politecnico di Milano, Piazza L. da Vinci, 32, 20133, Milano, Italy.*
**santosh.raavi@iit.it*

Abstract: We report on the ultrafast excited-state relaxation dynamics of the metastable photo-merocyanine (open-form) isomer of spiro-phenantroxazine, measured by pump and probe spectroscopy with sub-40-fs temporal resolution. We found that the photo-induced yield for ring-closure is negligible, and that the excited-state lifetime is only on the order of 300 fs. Relaxation leads to the non-adiabatic formation of a hot ground state (HGS). In this state, a coherent oscillation with 45 cm^{-1} frequency is present, showing strong anharmonicity. We attribute it to the motion (torsion/bending) of the molecular backbone attempting geometric relaxation to the close form. The strength of the coherent oscillation and the subsequent spectral relaxation in the HGS, together with the ultrashort lifetime, points to a crossing through a conical intersection (CI). We conclude that excited-states on the merocyanine form pass through a CI that is different from the one that would lead to ring-closure. We discuss design rules for the spiro-oxazine class, allowing for bidirectional switching avoiding this parasitic CI.

OCIS codes: (320.7150) Ultrafast spectroscopy; (160.2900) Optical storage materials; (160.4890) Organic materials.

References and Links

1. J. C. Crano and R. J. Guglielmetti, *Organic Photochromic and Thermochromic Compounds*, Kluwer Academic Publishers, New York, 2002.
2. E. Fischer and Y. Hirshberg, "Formation of coloured forms of spirans by low-temperature irradiation," J. Chem. Soc. **868**, 4522–4524 (1952).
3. N. Tamai and H. Miyasaka, "Ultrafast dynamics of photochromic systems," Chem. Rev. **100**(5), 1875–1890 (2000).
4. M. Garavelli, F. Bernardi, M. Olivucci, T. Vreven, S. Klein, P. Celani, and M. A. Robb, "Potential-energy surfaces for ultrafast photochemistry static and dynamic aspects," Faraday Discuss. **110**, 51–70 (1998).
5. B. G. Levine and T. J. Martínez, "Isomerization through conical intersections," Annu. Rev. Phys. Chem. **58**(1), 613–634 (2007).
6. D. R. Yarkony, "Diabolical conical intersections," Rev. Mod. Phys. **68**(4), 985–1013 (1996).
7. M. A. Robb, F. Bernardi, and M. Olivucci, "Conical intersections as a mechanistic feature of organic photochemistry," Pure Appl. Chem. **67**(5), 783–789 (1995).
8. H. Dürr, H. B-Laurent, *Photochromism: Molecules and Systems*, Elsevier, New York, 2003.
9. V. A. Lokshin, A. Samat, and A. V. Metelitsa, "Spirooxazines: synthesis, structure, spectral and photochromic properties," Russ. Chem. Rev. **71**(11), 893–916 (2002) (and references therein).
10. G. Berkovic, V. Krongauz, and V. Weiss, "Spiropyrans and spirooxazines for memories and switches," Chem. Rev. **100**(5), 1741–1754 (2000).
11. P. Andersson, N. D. Robinson, and M. Berggren, "Switchable charge traps in polymer diodes," Adv. Mater. (Deerfield Beach Fla.) **17**(14), 1798–1803 (2005).
12. S. Schneider, A. Mindl, G. Elfinger, and M. Melzig, "Photochromism of spirooxazines. 1. Investigation of the primary processes in the ring-opening reactions by picoseconds time-resolved absorption and emission spectroscopy," Ber. Bunsenges. Phys. Chem **91**, 1222 (1987).
13. S. Aramaki and G. H. Atkinson, "Spirooxazine photochromism: picosecond time-resolved Raman and absorption spectroscopy," Chem. Phys. Lett. **170**(2-3), 181–186 (1990).
14. N. Tamai and M. Masuhara, "Femtosecond transient absorption spectroscopy of a spirooxazine photochromic reaction," Chem. Phys. Lett. **191**(1-2), 189–194 (1992).

#145783 - $15.00 USD Received 12 Apr 2011; revised 20 May 2011; accepted 23 May 2011; published 27 May 2011

15. S. A. Antipin, A. N. Petrukhin, F. E. Gostev, V. S. Marevtsev, A. A. Titov, V. A. Barachevsky, Yu. P. Strokach, and O. M. Sarkisov, "Femtosecond transient absorption spectroscopy of non-substituted photochromic spirocompounds," Chem. Phys. Lett. **331**(5-6), 378–386 (2000).
16. F. Maurel, J. Aubard, P. Millie, J. P. Dognon, M. Rajzmann, R. Guglielmetti, and A. Samat, "Quantum chemical study of the photocoloration reaction in the napthoxazine series," J. Phys. Chem. A **110**(14), 4759–4771 (2006).
17. G. Buntinx, S. Foley, C. Lefumeux, V. Lokshin, O. Poizat, and A. Samat, "Evidence for a photophysical deactivation pathway competing with the photochromic transformation in a cyano-substituted spironaphthoxazine," Chem. Phys. Lett. **391**(1-3), 33–37 (2004).
18. M. Suzuki, T. Asahi, and H. Masuhara, "Photochromic reactions of crystalline spiropyrans and spirooxazines induced by intense femtosecond laser excitation," Phys. Chem. Chem. Phys. **4**(2), 185–192 (2002).
19. M. Suzuki, T. Asahi, and H. Masuhara, "Cooperative photochemical reaction mechanism of femtosecond laser-induced photocoloration in spirooxazine microcrystals," ChemPhysChem **6**(11), 2396–2403 (2005).
20. G. Favaro, V. Malatesta, U. Mazzucato, G. Ottavi, and A. Romani, "Thermally reversible photoconversion of spiroindoline-naphthooxazines to photomerocyanines: a photochemical and kinetic study," J. Photochem. Photobiol. Chem. **87**(3), 235–241 (1995).
21. A. Chibisov and H. Görner, "Photoprocesses in spirooxazines and their merocyanines," J. Phys. Chem. A **103**(26), 5211–5216 (1999).
22. J. Buback, M. Kullmann, F. Langhojer, P. Nuernberger, R. Schmidt, F. Würthner, and T. Brixner, "Ultrafast bidirectional photoswitching of a spiropyran," J. Am. Chem. Soc. **132**(46), 16510–16519 (2010).
23. I. Gómez, M. Reguero, and M. A. Robb, "Efficient photochemical merocyanine-to-spiropyran ring closure mechanism through an extended conical intersection seam. A model CASSCF/CASPT2 study," J. Phys. Chem. A **110**(11), 3986–3991 (2006).
24. G. Cerullo and S. De Silvestri, "Optical parametric amplifiers," Rev. Sci. Instrum. **74**(1), 1–18 (2003).
25. D. Polli, D. Brida, S. Mukamel, G. Lanzani, and G. Cerullo, "Effective temporal resolution in pump-probe spectroscopy with strongly chirped pulses," Phys. Rev. A **82**(053809), 1–8 (2010).
26. L. Lüer, C. Manzoni, G. Cerullo, G. Lanzani, and M. Meneghetti, "Ultrafast dynamics of a charge-transfer dimmer as a model for the photoinduced phase transition of charge-tranfer compounds," Phys. Rev. Lett. **99**(027401), 1–4 (2007).
27. D. Polli, P. Altoè, O. Weingart, K. M. Spillane, C. Manzoni, D. Brida, G. Tomasello, G. Orlandi, P. Kukura, R. A. Mathies, M. Garavelli, and G. Cerullo, "Conical intersection dynamics of the primary photoisomerization event in vision," Nature **467**(7314), 440–443 (2010).
28. Q. Wang, R. W. Schoenlein, L. A. Peteanu, R. A. Mathies, and C. V. Shank, "Vibrationally coherent photochemistry in the femtosecond primary event of vision," Science **266**(5184), 422–424 (1994).

1. Introduction

Photochromism - a reversible photoinduced transition between two forms of a chemical species, entailing strong persistent changes in physical properties - is intensively studied because of its many applications in molecular photonics, particularly in the construction of ultra high density three-dimensional memories and optical switches [1,2]. Molecular rearrangements in chemical reactions usually occur on a time scale comparable to nuclear vibrational periods (i.e., from 10 fs to 1 ps). Therefore, spectroscopic methods with high temporal resolution are required to study the photo-physics of photochromic molecules. Time resolved studies suggest that the initial step of a photochromic reaction proceeds on a sub-ps time scale and more importantly along a singlet excited-state pathway [3]. Due to its ultrashort character and the high energy deposited by the excitation pump in the molecular wavepacket, its evolution cannot be simply described using an equilibrium state-to-state pathway, as it will rather follow an adiabatic path determined by the complex interplay of the initial photo-processes and the vibrational energy redistribution. From theoretical calculations [4] it was shown that the first excited-state potential energy surface (called S_1 in the following) is characterized by two domains: one at high energy (close to the Franck-Condon region) that controls the initial wavepacket acceleration and another at low energy that determines the relaxation back to the ground state. Most often in photochromic molecules the ground state (S_0) potential energy surfaces (PES) and S_1 display a conical intersection (CI) [5–7] in the vicinity of the Franck-Condon region, which strongly influences the overall properties of the considered photochromic compounds.

Spirooxazines (SO) are photochromic molecules whose substituted derivatives have been extensively studied [1,2,8–10]. SO are composed of two weakly interacting orthogonal heterocyclic fragments, linked through an sp^3 carbon atom, and absorb in the UV region. Upon UV irradiation, the relatively weak linking between the sp^3 carbon atom and the oxygen atom of the parent SO molecule experiences bond cleavage [2], that leads to the rotation about

#145783 - $15.00 USD Received 12 Apr 2011; revised 20 May 2011; accepted 23 May 2011; published 27 May 2011

the C-O bond resulting in the flattened, open-ring and colored isomer which is known as photo-merocyanine (PMC). PMCs are thermally unstable, leading to the back reaction to the SO form even in the dark. Owing to the extended conjugation of the π-electron system of PMC, it exhibits a characteristic ground state absorption (GSA) band in the visible wavelength region peaking at 585nm (see the red solid line in Fig. 1). SOs has been extensively applied in memories and switches [10,11] due to their excellent resistance to light-induced degradation. Earlier works on the SO ring-opening mechanism and dynamics [3,12–21] show that the C–O bond cleavage occurs in ps to sub-ps time scales and it proceeds through the formation of an intermediate photoproduct, called X, having orthogonal parent geometry. Using transient absorption experiments Antipin *et al.* [15] estimated the rate constants of different intermediates to be approximately $(100\ \text{fs})^{-1}$, $(300\ \text{fs})^{-1}$ and $(2000\ \text{fs})^{-1}$, eventually leading to the formation of the final trans-PMC photoproduct. The existence of an X state has later been challenged by a theoretical paper, showing that the experimental findings of ref [15]. are consistent with a local minimum on the ground state PES, associated with the cis-PMC [16]. The authors predict that the activation barrier for the cis-trans isomerization in the ground state controls the photochromic ring-opening yield.

The key mechanism involved in the use of photochromic systems for memory and logic devices is the possibility of obtaining bidirectional optical switching. Chemical substitution, for example, by push-pull-substituents, has allowed the increase of the ring-closure yield, however on the expense of reducing the ring-opening yield [22]. It seems that thermodynamically stabilizing the merocyanine form increases the photochromic ring-closure yield, but general design rules to achieve high ring-closure yields are not yet available. Photo-induced ring-closure has been studied on the CASSCF/CASPT2 level of theory in a simple model system [23]. A two-step mechanism was proposed by which ultrafast trans-cis isomerization is followed by ring-closure through a CI. A complete cycle of ring-closure and opening has been demonstrated to evolve in 6 ps in a spiropyran derivative [22]. According to these theoretical and experimental findings, the ring-closure yield should be related to the probability to reach the CI involved in the final ring-closure step. Possible inhibitors are energetic barriers or additional "parasitic" CIs. The distinction between these two possibilities can be done by measuring the excited-state lifetimes of the PMC form in the case of low ring-closure yields: excited-state lifetimes in the upper picosecond range demonstrate the presence of barriers, while sub-picosecond lifetimes point to the presence of parasitic CIs. The characterization of the inhibitor to ring-closure will yield design principles to obtain high yields for bidirectional optical switching.

Here, we report on the excited-state dynamics of the PMC species of SO of which we provide a stationary excess concentration by CW irradiation with UV light (see next section). We found that the yield for photo-induced ring-closing is near to zero. Transient differential transmission spectra reveal, for the first time to the best of our knowledge: (a) stimulated emission from the $S_1 \rightarrow S_0$ state decaying within 300 fs, and (b) the fast formation of a hot ground state in which the geometric distortion undergone in the excited-state is slowly relaxed through a torsion/bending motion of the molecular backbone which shows up as a slow coherent oscillation with 45 cm^{-1} frequency. The studies presented here also demonstrate that the low efficiency of back conversion of PMC to SO form is due to presence of parasitic CI.

2. Experimental details

The spiroxazine under study is a substituted spirophenantrooxazine molecule: 1,3-Dihydro-1,3,3-trimethylspiro[2H-indole-2,3′-[3H]phenanthr [9,10b](1,4)oxazine]. It has been purchased from Sigma Aldrich and used without further purification in spectrophotometric-grade toluene solution with 5×10^{-4} M molar concentration. The closed-ring structured parent spirooxazine molecule is referred to as "Form A" in the following and the photoproduct open-structured species is referred to as Form B (see Fig. 1 for the molecular structures). In solution, there is always equilibrium between Form A and the metastable Form B [9]; however one can enhance the concentration of Form B by virtue of continuous irradiation of

#145783 - $15.00 USD Received 12 Apr 2011; revised 20 May 2011; accepted 23 May 2011; published 27 May 2011

Form A with a wavelength shorter than 400 nm. In the present case of the molecule under study, the quantum-yield of the photo-isomerization from Form A is ≈0.49 in toluene solution when excited with 354 nm [20]. For this reason, we constantly excite the sample volume around the pump-probe overlap region with a low-power continuous-wave UV beam at 375-nm wavelength from a diode laser (from Micron Inc., Model LDM 375-20 cwA). We observe an increment of the absorption band centered on 585nm upon increasing the UV intensity, confirming that we can significantly augment the concentration of Form B for our experiment. Furthermore, since we are pumping at 580 nm where only the closed Form B absorbs (see Fig. 1), the resulting pump-probe spectra will solely contain information about Form B. The sample is placed in a quartz cuvette (Hellma 121-0.50-40) with 500 μm optical path length.

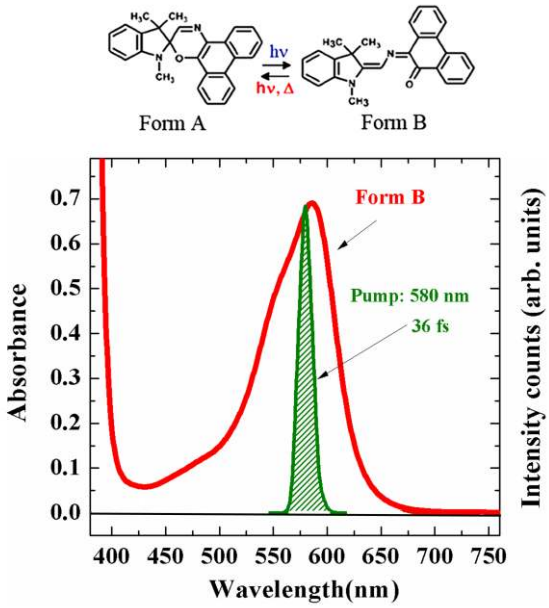

Fig. 1. (a) Molecular structure of the molecule under study, and (b) absorbance spectrum of the Form B species. The shaded region represents the pump-pulse used in the experiment.

The pump-probe set-up is based on a commercial Ti:Sapphire regeneratively amplified laser system (Quantronix model Integra-C), delivering 1-mJ pulses at 1-kHz repetition rate at 800-nm center wavelength with ≈150-fs duration. A fraction of the fundamental beam (≈150μJ) is used to pump a non-collinear optical parametric amplifier (NOPA) delivering ultra-broadband pulses in the visible with spectrum spanning the 500–700 nm wavelength region. The details of NOPA used can be found elsewhere [24]. For these experiments we tuned the NOPA in order to deliver narrow-band pump pulses with a central frequency at 580 nm as shown in Fig. 1. Careful dispersion compensation (also considering the cuvette glass windows) guarantees an almost transform-limited pump duration of ≈36 fs on the sample. The probe pulses are obtained by focusing a portion of the fundamental beam (with ≈2 μJ energy) into a 1-mm-thick sapphire plate to generate a stable single-filament white-light supercontinuum. A short-pass filter with 760 nm cutoff wavelength is used to filter out the residual 800 nm pump and the infra-red component of the probe pulses, thus limiting our probing window to the 450-750 nm spectral region. The white-light is not compressed and results in a highly chirped probe pulse with ≈400 fs overall duration. Nonetheless, using a spectrometer to detect the probe pulses, it has been possible to obtain an observation window of ≈10 fs, thus preserving an effective temporal resolution of ≈37 fs [25]. The measured signal is a two-dimensional map of the differential transmission $\Delta T/T(\lambda,\tau) = [(T_{on}-T_{off})/T_{off}]$ as a function of probe wavelength (λ)

#145783 - $15.00 USD Received 12 Apr 2011; revised 20 May 2011; accepted 23 May 2011; published 27 May 2011

and delay (τ), where T_{on} and T_{off} are the probe spectra transmitted by the excited and unperturbed sample, respectively. All the measurements were performed using ≈12 μJ/cm^2 incident pump fluence at room temperature.

3. Results

Figure 2 shows the measured ΔT/T spectra of Form B pumped at 585nm at selected probe delays in the visible wavelength range. The nascent spectra show a positive band (green area), peaking at 585 nm. This positive (increased transmission) band corresponds to photo-bleaching (PB) of the ground state caused by the absorption of pump photons to the first excited-state S_1. This band is narrower compared to the GSA spectral profile (see Fig. 1) even at 4.5 ps delay, most likely due to a hole burning effect in the inhomogeneously broadened GSA, which is wider than the pump pulse spectrum.

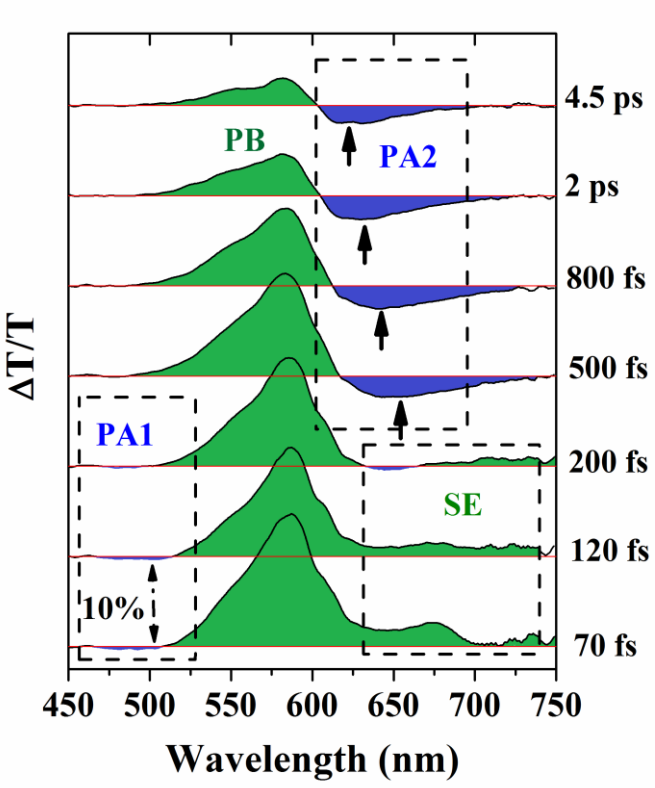

Fig. 2. ΔT/T spectra at various probe delays for Form B pumped at 580 nm; the positive region (green) represents the PB and SE spectral bands, while the negative regions (blue) correspond to the two PA signals; the arrows highlight the gradual blue shift of the peak of the PA2 signal.

At the blue and red sides of PB we observe two negative ΔT/T bands due to photo-induced absorption (PA) from the excited S_1 state to higher-lying singlet states. One is visible at 460-520 nm (called PA1 in the following) and the other at 610-750 nm (PA2). Further, within the first 300 fs, we see another positive band extending after 650 nm until the end of our spectral observation window. As Form B doesn't present any absorption in this wavelength region, we assign it to stimulated emission (SE), representing the $S_1 \rightarrow S_0$ radiative decay. Figure 3 shows the details of the spectral evolution in the first 400 fs in which we observe the most interesting primary photo-events after the photo-excitation of Form B. Figure 3(a) indicates that the instantaneously formed PA1 rapidly decays and evolves into the PB within ≈300 fs whereas in the meanwhile the SE signal decays and simultaneously red-shifts towards the NIR/IR region (beyond our spectral observation window) as shown in Fig. 3(b). In contrast to the observed

#145783 - $15.00 USD Received 12 Apr 2011; revised 20 May 2011; accepted 23 May 2011; published 27 May 2011

fast processes, PA2 is not present at early time delays but it forms on a 300-fs time scale, followed by a gradual blue shift until 5 ps, as highlighted by the arrows in Fig. 2.

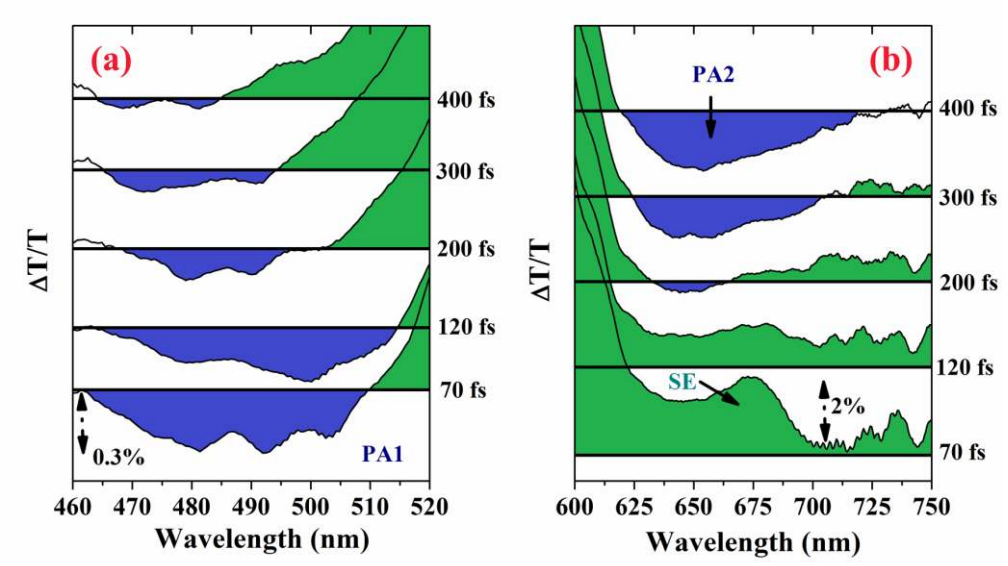

Fig. 3. ΔT/T spectra in the first 400 fs; (a) rapid decay of 460-510 nm spectral region (PA1) within 400 fs; (b) spectral evolution in the 620-750 nm showing rapid decay of SE decaying leading to the formation of PA2.

We show in Fig. 4 the ΔT/T dynamics at selected probe wavelengths chosen as representative of the various processes described in the discussion above. The experimental data is plotted as dotted black curve while the solid red line represents the results obtained from the global fitting of the experimental data as discussed in the next section. Figure 4 shows the ΔT/T dynamics at (a) 485 nm displaying the rapid decay of PA1; (b) 500 nm representing the temporal evolution of the region in PA1 that in a few hundreds of femtoseconds it turns into a positive signal due to PB of the GSA; (c) 585 nm, showing PB at the GSA maximum, with a multi-exponential decay (as discussed later), leading to a complete PB recovery within ≈100 ps (not shown here). The temporal evolution of PA2 is evident from Figs. 4(d - e), where the measured ΔT/T signals at 620 and 650 nm probe wavelengths showing a change in sign from PB to PA2 at 700 and 300 fs delays, respectively. On a picosecond time scale, PA2 undergoes a considerable blue shift, as it can be estimated from the probe wavelength dependent time of maximum PA, being 0.6, 1.2, and 1.8 ps for 680, 650, and 620 nm, respectively. As evident from Fig. 1, the Form B species displays a very small absorption tail at till ≈650 nm with no absorption at λ>670 nm. Therefore, we assign the positive feature at early probe delays in the ΔT/T signal at 650 nm (panel (e)) to a combination of PB and SE while that at 680 nm (panel (f)) to pure SE.

#145783 - $15.00 USD Received 12 Apr 2011; revised 20 May 2011; accepted 23 May 2011; published 27 May 2011

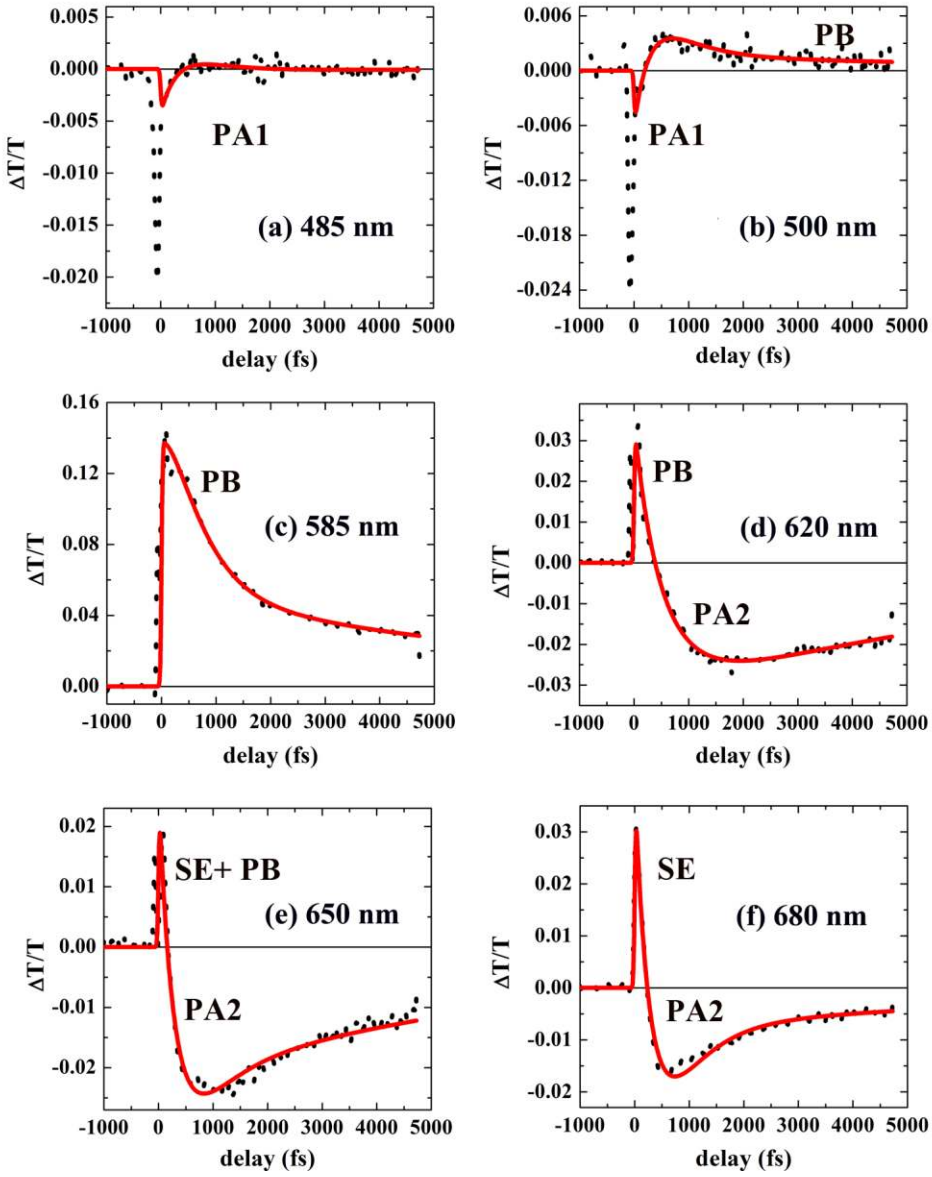

Fig. 4. ΔT/T dynamics at selected probe wavelengths. The black dotted line represents the experimental data while the red solid line represents the calculated fits using the modeling described in the section 4.1

4. Discussion

Though the Form B species are PMC product of spirooxazine molecule, the experimental conditions used here conveniently allow us to probe only the Form B. The presence of PB corresponding to the spectral region of GSA of the Form B in the overall probe delay confirms that we only probe the photo-excited states of Form B reached after resonantly pumping at 580 nm. The temporal dynamics of ΔT/T signals at 680 nm (SE) and 485 (PA1) showing similar kinetic behavior as seen in Fig. 4 and the spectral evolution of PA1 and SE (see Fig. 3) clearly confirm that the PA1 is a photo-induced absorption of the S_1 state. The formation of PA2, red-shifted against PB by a displacement ΔE which is reduced to values

#145783 - $15.00 USD Received 12 Apr 2011; revised 20 May 2011; accepted 23 May 2011; published 27 May 2011

below the band widths within a few picoseconds, indicates the rapid evolution of the population into a HGS, undergoing thermalization on a time-scale typical for organic conjugated systems in a "bath" [26]. In fact, in spite of strong persistent PB and PA features in the picosecond region, the spectrally integrated differential absorption decays to a value close to zero within 1 ps (data not shown). This is a strong argument for PB and PA sharing different vibronic manifolds of the same state, leading in the pump-probe spectra only to redistribution of oscillator strength, but with zero integral. It is known [12–15] that upon resonant excitation of closed-ring SO molecule (Form A) with λ<400 nm, the evolution of the ring-opening mechanism proceeds via S_1 of the Form A having a peak at ≈490 nm. From Fig. 3, we notice that the PA1 band has the local maximum at a similar spectral position. However, only from this coincidence it cannot be concluded that these PA bands refer to the same excited-state geometry, which would be in fact a contradiction with the model above. Due to strong overlap with the PB features and the spectral detection window extending up to 450 nm, the real position of the PA1 center cannot be known with sufficient precision in our case.

The observation of a strong progressive red shift of SE over the first 200 fs points to a strong gradient of the S_1 state in the Frank Condon region, inducing rapid wavefunction propagation towards a region with strongly reduced energy difference between S_0 and S_1. This strong wavefunction propagation is confirmed by the observation of significant spectral relaxation in the HGS, and by the occurrence of coherent oscillations (sees next section). Such a strong gradient is usually caused by a nearby CI, which therefore tends to "attract" the excited-state wavepacket. In fact, the very short excited-state lifetime of only 300 fs is a strong indication that the excited-state wavepacket swiftly encounters a CI. It is tempting to conclude that S_1 states formed in either Form A or Form B, must pass through the same CI. However, at this point, we highlight our observation of vanishing PB after a few picoseconds, showing that the quantum yield for photoinduced ring-closure is negligible. This differs from exciting the closed-ring molecule (Form A), where the quantum yield is ≈0.49. Moreover, exciting the closed-ring parent spirooxazine molecule leads to a clearly different dynamics. Antipin *et.al.,* [15] showed the occurrence of an intermediate state, which has an absorption at around 500 nm, stable for several hundred femtoseconds, after which the hot ground state is formed on a picosecond time scale. In our measurements, after pumping the Form B, there is no indication of such a metastable intermediate, and the formation of the hot ground state is much more rapid than after pumping Form A. In summary, the comparison with our work to ref [15] shows that after pumping Form B in our molecule, a CI is reached which is different from the one reached by Form A excited-states.

The observation of a second CI is an important clue for material optimization. The stable intermediate, reported in ref [15], has been assigned to the cis-form of PMC, forming a local minimum on the ground state PES with a significant energy barrier towards the final trans-forms. Our CI is expected to refer to a transoid geometry. Hence, the HGS, formed after pumping the Form B, does not evolve far enough to the cisoid geometry, which is needed to get back to the Form A with significant quantum yield. It is known that CIs frequently occur when torsion around one conjugated double bond introduces a conjugation break. Once the torsion angle between the two isolated conjugated systems reaches 90°, S_0 and S_1 become degenerate because of their biradical nature [16]. If the parasitic CI, that we observe here, is caused by the rotation about a double bond, then the "driving force" towards the CI – the energy gain by increasing the torsional angle - can be reduced by push-pull substituents that reduce the wavefunction coefficients of the double bond in question in the LUMO. This picture is consistent with the fact that Buback *et al.* [22], obtained a high closure yield. It would be interesting to identify which of the double bonds causes the parasitic CI that we observed. This can however not be done on a quantitative level, like, a simple one-configuration-scheme considering only the frontier orbitals. Only a multi-reference quantum chemical calculation can treat correctly near-degenerate states. Moreover, knowledge of the bond length alternation and its change when going from S_0 to S_1 is essential to correctly describe torsion-induced PES. This work is therefore an important input for the

#145783 - $15.00 USD Received 12 Apr 2011; revised 20 May 2011; accepted 23 May 2011; published 27 May 2011

comprehensive quantum-chemical calculation of the S_0 and S_1 PES in the vicinity of the PMC in both systems.

4.1 Global fitting

From the observed data we propose the following scenario: (i) Upon photo-excitation to the S_1 state the system relaxes in ≈300 fs (as detected by monitoring the PA1 band at λ<510 nm) and ultrafast internal conversion brings the system to the HGS; (ii) no conversion to the open Form A is observed as we do not see any long-lived PB of the Form B; (iii) the HGS thermalizes towards equilibrium (S_0), consistent with a blue shift of the PA in the 600-700 nm spectral band. To explain the observed photo-physical behavior of the transient spectra we consider a model based on three (electronically or vibronically) excited-states called S_1, $S_{01\text{-hot}}$ and $S_{0\text{-hot}}$ and the ground state S_0 connected via a sequential reaction scheme and performing global fitting using the following rate equations:

$$\frac{dN_0(t)}{dt} = -gen(t) + k_3 N_3(t), \tag{1}$$

$$\frac{dN_1(t)}{dt} = gen(t) - k_1 N_1(t), \tag{2}$$

$$\frac{dN_2(t)}{dt} = k_1 N_1(t) - k_2 N_2(t), \tag{3}$$

$$\frac{dN_3(t)}{dt} = k_2 N_2(t) - k_3 N_3(t), \tag{4}$$

$$\frac{dT(t,\lambda)}{T} \approx dA = S_1(\lambda) N_1(t) + S_{01-hot}(\lambda) N_2(t) + S_{0-hot}(\lambda) N_3(t), \tag{5}$$

where N_0, N_1, N_2 and N_3 describe the population in S_0, S_1, $S_{01\text{-hot}}$ and $S_{0\text{-hot}}$, respectively, and *gen(t)* is the temporal profile of the pump pulse with 37 fs FWHM duration. It is important to note that the spectral changes, which we found experimentally, are indicative of a continuous relaxation of the excited-state wavepacket, as distinguished from a short-lived but stable intermediate. In consequence, the "basis spectra", that are obtained by a global fitting approach, do not represent eigen-functions on local or global minima of the respective PES, but rather represent typical positions of the wavepacket during their course of full relaxation. The global fitting scheme yields the full photoinduced spectra of the excited-states S_1, $S_{01\text{-hot}}$ and $S_{0\text{-hot}}$, including PA to higher states, SE to the ground state and the PB contribution of each state (see red solid curves in Fig. 4).

We find excellent agreement with the measured temporal dynamics of ΔT/T signals at all probe wavelengths representing various spectral features (black dashed curves in Fig. 4). The simulated basis-spectra and their population-decay dynamics are presented in Fig. 5(a) and (b) respectively. The spectral features of the photoexcited spectra are photophysically reasonable and help us to locate the states of the PES. The first photo-excited state spectrum reached after photo-excitation of S_1 (see red curve in Fig. 5(a)) resembles the ΔT/T spectrum measured around time zero, when the wavepacket is still close to the Frank-Condon region and thus the main portion of SE is still in the visible spectral region: its main features are PB at the spectral position of the steady-state GSA, PA1 band (shown as a small negative signal around 500 nm) and a small peak around 680 nm representing the SE. The S_1 state decays with a time constant of $1/k_1$ = 285 fs (see red curve in Fig. 5(b)) into the vibronically hot ground state $S_{01\text{-hot}}$ (see green dashed curve in Fig. 5(a)) characterized by PB which closely resembles the GSA and a broad photo-induced absorption PA2 at wavelengths longer than 610 nm, where S_1 showed SE. Based on the spectral proximity of PA2 and PB, and the absence of other PA bands, PA2

#145783 - $15.00 USD Received 12 Apr 2011; revised 20 May 2011; accepted 23 May 2011; published 27 May 2011

is thus identified as a hot (and therefore red-shifted) ground state absorption. Since PA2 extends strongly into the red, we conclude that $S_{01\text{-hot}}$ is still very close to the crossing point between S_1 and S_0 Within $1/k_2$ = 550 fs (see green curve Fig. 5(b)), $S_{0\text{-hot}}$, is reached which is characterized by PB and the PA2 which are substantially overlapped and show similar spectral weight (see blue curve in Fig. 5(a)). The PA2 in $S_{0\text{-hot}}$ is strongly blue-shifted and narrowed in comparison with the PA2 in $S_{01\text{-hot}}$. This state relaxes to the fully thermalized ground state S_0 within $1/k_3$ = 7.6 ps, see blue curve in Fig. 5(b)) with only minor spectral changes, corresponding to an excess energy ($\Delta\varepsilon$) of a few times kT.

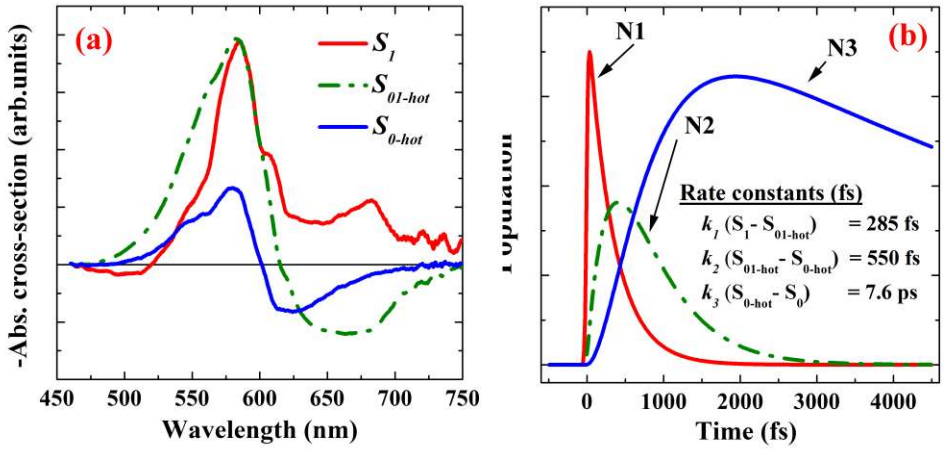

Fig. 5. (a) Basis spectra obtained from the global fitting procedure; (b) the decay dynamics of the different species with the rate constant.

4.2 Coherent phonon dynamics

We observed the presence of intense periodic modulations superimposed on the time traces. In order to analyze them in detail, we isolated them by subtracting the slowly-varying population dynamics from the measured $\Delta T/T$ data. The results at 565 and 650 nm probe wavelengths are plotted in Fig. 6(a). The residuals clearly show coherent oscillations in counter-phase. By Fourier-transform of the time traces at each probe wavelength, we find that the wavenumber spectrum is dominated by a mode at 45 cm^{-1} frequency. The modulation depth profile, as plotted in Fig. 6(b), shows a minimum at 620 nm, where there is also a π phase jump. This identifies rather clearly the coherent signal as being associated to wavepacket oscillation around an optical resonance at 620 nm. Since the GSA spectrum peaks at 580 nm, we can clearly rule out ground state coherence. Furthermore, such ground state coherence should be negligible because due to the large difference between pump pulse duration (≈36 fs) and vibrational period (≈740 fs) the impulsive stimulated Raman process is not active. We associate the coherent oscillation to a wavepacket motion in the HGS, because a subtraction of the PB contribution to the optical spectrum of the $S_{01\text{-hot}}$ in Fig. 6(a) yields a PA maximum at about 620 nm (see also PA2 in the $\Delta T/T$ spectrum in Fig. 2). Such coherent wavepacket has initially been created in S_1 and it then coherently proceeds through the CI down to the PES of HGS. As the oscillation has a period of 740 fs, a stochastic process involving the immediate transition of S_1 into the HGS that occurs in 300 fs cannot completely destroy coherence since such a fast transition is known to occur non-adiabatically through the presence of CI preserving the coherence of the excited wavepacket. This has already been observed in the photophysics of rhodopsin, where the excited wavepacket maintains its coherence passing through the CI and reaches the photo-product ground state where oscillations with 500-fs period are seen [27,28]. This oscillation tells us the main reorganization path after the CI

#145783 - $15.00 USD Received 12 Apr 2011; revised 20 May 2011; accepted 23 May 2011; published 27 May 2011

down to the relaxed Form B ground state, serving as important input for a quantum-chemical calculation of vibrational frequencies in the ground state of this molecule with high accuracy.

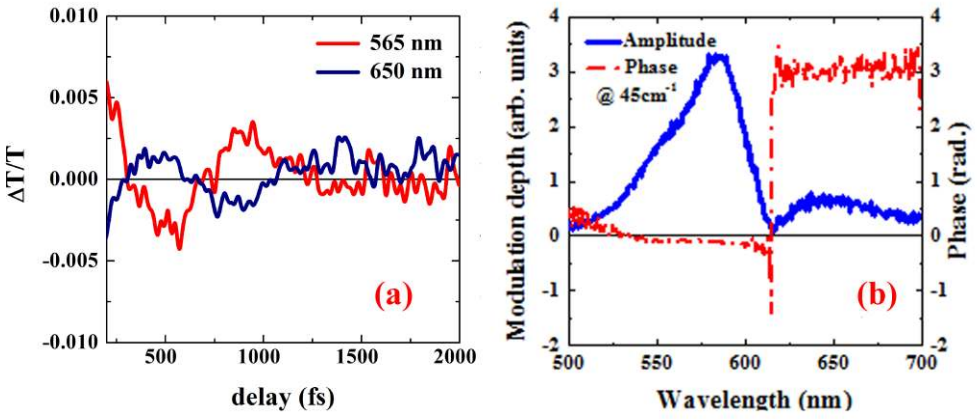

Fig. 6. (a) Typical ΔT/T time traces after removal of the exponential decay term, showing oscillatory patterns having opposite phase; (b) amplitude (blue solid curve) and phase (red dash-dot curve) of fourier-transform spectra at 45 cm^{-1} frequency.

4.3 Proposed PES picture

In Fig. 7 we show the ingredients for a PES model around the PMC geometry that can be deduced from our experiments. Our scheme is adapted the one shown by Buback *et al* [22]. The thermodynamically stable form is the trans-PMC. After resonantly pumping the S_1 state with some excess energy, the energy barrier between the trans- and cis- geometries can be overcome. The actual ring-closure occurs in the S_1 state of the cis-PMC passing through a C.I. Note that a theoretical paper by Gomez *et al.* [23], done on the smallest possible model compound for ring-closure, found that the primary photoexcitation of the PMC is the S_2 state, because the $S_0 \rightarrow S_1$ transition is of n-π character and thus only weakly allowed. We note however that the non-bonding character is expected to decrease upon extension of the π-conjugated system, and therefore we assume S_1 as our primary excited-state, in accordance with ref [22] and with our own experimental evidence.

Summarizing our experimental findings, (i) excited-state lifetime is only a few hundred femtoseconds and (ii) our ring-closure yield is close to zero. A short excited-state lifetime could be explained by a lowering of the trans-cis barrier. But then the expected ring-closure yield should be high, because a wavepacket arriving from the PMC side possesses the quantum-chemical equivalent of "inertia", so that after going through the CI, it will continue its propagation into the same direction as before, that is, towards the Form A. Vice versa, a low ring-closure yield could be explained by a high trans-cis barrier. But then, the ultrashort excited-state lifetime cannot be explained. The only model consistent with both experimental observations is the presence of an additional "parasitic" CI along a different coordinate (depicted by dashed lines in Fig. 7). In conclusion, the ring-closure yield in the presence of this parasitic CI is governed by the probability for the wavepacket to cross the trans-cis barrier before being attracted by this additional CI. This notion gives organic synthesizers two handles towards high ring-closure yields: (i) lowering the trans-cis barrier; however this might be detrimental for the ring-opening yield. (ii) Making the parasitic CI energetically more "S_1-like", meaning that the conformational change that leads to the CI should be more or less neutral to the S_1 energy. In this case, wave-function propagation towards this CI will be weak.

#145783 - $15.00 USD Received 12 Apr 2011; revised 20 May 2011; accepted 23 May 2011; published 27 May 2011

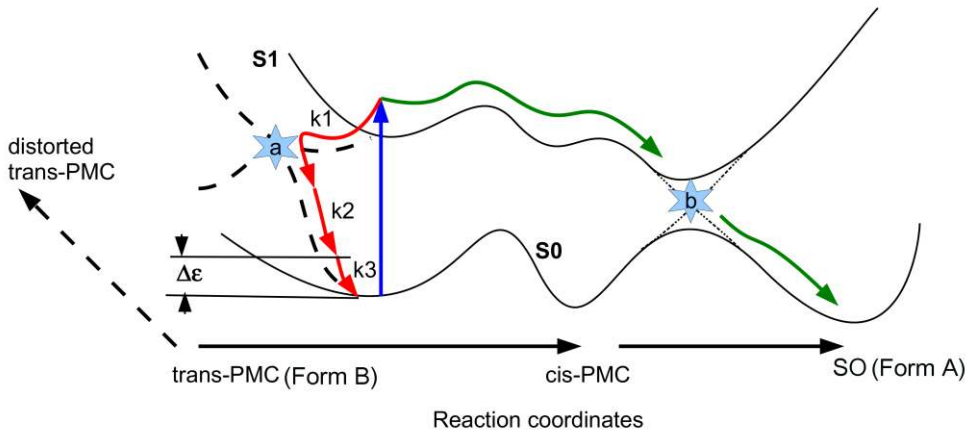

Fig. 7. : Proposed scheme of the PES model for the photo-chemical reaction, adapted from [23] CIs are given as star-shaped objects.The pathway of a successful ring- closure is given by black curvy arrows, crossing through the "useful" CI "b" that connects the spiro and cis-PMC forms. Unsuccessful attempts to close the ring pass through a "parasitic" CI "a" along an additional reaction coordinate (dashed lines) that causes sub-picosecond excited-state relaxation and leads to a HGS, in agreement with our experimental findings

5. Conclusions

The primary spectral dynamics of the open form (PMC) of spiro-phenantroxazine is studied using sub-40 fs pump-probe spectroscopy. We observed negligible yield for photoinduced ring-closure after an excited-state lifetime of only 300 fs. We conclude that in this molecule, the excited-state wavepacket passes through a "parasitic" CI which is different from the one that leads to ring- closure and which leads to a frustrated reaction. A slow coherent oscillation of 45 cm^{-1} is observed suggesting a molecular backbone motion (torsion/bending) attempting geometric relaxation to the closed-form though the molecule fails to form the closed-ring structure completely and return to the open-form. These findings have implications on the synthetic strategy to yield effective bidirectional switching, encouraging trans-cis isomerization before this additional "parasitic" CI is encountered by the excited-state wavepacket.

Acknowledgments

Authors acknowledge Josh Holt, Daniele Brida for their contribution in software used for the data/kinetic modeling. LL and GL thank the support of the European Commission, grant Nr MRTN-CT-2006-035859BIMORE. DP thanks financial support from Human Frontier Science Program Organization under the project number RGP0005 and the Politecnico di Milano under the project "Understanding the Architecture of Photosynthetic Light Harvesting by Space and Time Resolved Spectroscopy".

#145783 - $15.00 USD Received 12 Apr 2011; revised 20 May 2011; accepted 23 May 2011; published 27 May 2011